Experimental measurement of the dispersion relations of the surface plasmon modes of metal nanoparticle chains

K. B. Crozier*, E. Togan, E. Simsek, and T. Yang

School of Engineering and Applied Sciences, Harvard University, Cambridge, MA, USA
**Corresponding author: kcrozier@seas.harvard.edu*

Abstract: The dispersion relations of the surface plasmon modes of metal nanoparticle chains are measured, and compared with theory. The theoretical model includes the effects of retardation, radiative damping and dynamic depolarization due to the finite size of the nanoparticles. The results reveal that, in addition to one longitudinal and one transverse mode, there is a third mode, which has not been previously reported.

OCIS codes: (220.4000) Microstructure fabrication; (240.6680) Surface Plasmons

References and links

1. B. E. Saleh and M. C. Teich, *Fundamentals of Photonics* (Wiley, New York, 1991).
2. J. Takahara, S. Yamagishi, H. Taki, A. Morimoto, and T. Kobayashi, "Guiding of a one-dimensional optical beam with nanometer diameter," Opt. Lett. **22**, 475-7 (1997).
3. M. Quinten, A. Leitner, J. R. Krenn and F. R. Aussenegg, "Electromagnetic energy transport via linear chains of silver nanoparticles," Opt. Lett. **23**, 1331-1333 (1998).
4. M. L Brongersma, J. W. Hartman, and H. A. Atwater, "Electromagnetic energy transfer and switching in nanoparticle chain arrays below the diffraction limit," Phys. Rev. B **62**, R16356-16359 (2000).
5. S. A. Maier, P. G. Kik and H. A. Atwater, "Observation of coupled plasmon-polariton modes in Au nanoparticle chain waveguides of different lengths: Estimation of waveguide loss," Appl. Phys. Lett. **81**, 1714-1716 (2002).
6. C. Girard and R. Quidant, "Near-field optical transmittance of metal particle chain waveguides," Opt. Express **12**, 6141-6146 (2004).
7. A. F. Koenderink and A. Polman, "Complex response and polariton-like dispersion splitting in periodic metal nanoparticle chains," Phys. Rev. B **74**, 033402-1-4 (2006).
8. V. A. Markel, "Coupled-dipole approach to scattering of light from a one-dimensional periodic dipole structure," J. Mod. Opt. **40**, 2281-2291 (1993).
9. A. L. Burin, H. Cao, G. C. Schatz, and M. A. Ratner, "High-quality optical modes in low-dimensional arrays of nanoparticles: application to random lasers," J. Opt. Soc. Am. B **21**, 121-131 (2004).
10. M. Guillon, "Field enhancement in a chain of optically bound dipoles," Opt. Express **14**, 3045-3055 (2006).
11. S. Zou and G. C. Schatz, "Narrow plasmonic/photonic extinction and scattering lineshapes for one and two dimensional silver nanoparticle arrays," J. Chem. Phys. **121**, 12606-12612 (2004).
12. C. R. Simovski, A. J. Viitanen, and S. A. Tretyakov, "Resonator mode in chains of silver spheres and its possible application," Phys. Rev. E **72**, 066606-1-10 (2005).
13. R. Quidant, C. Girard, J. C. Weeber, and A. Dereux, "Tailoring the transmittance of integrated optical waveguides with short metallic nanoparticle chains," Phys. Rev. B **69**, 085407-1-7 (2004).
14. K. Li, M. I. Stockman, and D. J. Bergman, "Self-similar chain of metal nanospheres as an efficient nanolens" Phys. Rev. Lett. **91**, 227402-1-4 (2003).
15. K. B. Crozier, A. Sundaramurthy, G. S. Kino and C. F. Quate, "Optical antennas: resonators for local field enhancement," J. Appl. Phys. **94**, 4632-4642 (2003).
16. A. Sundaramurthy, K. B. Crozier, G. S. Kino, D. P. Fromm, P. J. Schuck and W. E. Moerner, "Field enhancement and gap-dependent resonance in a system of two opposing tip-to-tip Au nanotriangles," Phys. Rev. B **72**, pp. 165409-1-6 (2005).
17. E. Cubukcu, E. A. Kort, K. B. Crozier, F. Capasso, "Plasmonic Laser Antenna," Appl. Phys. Lett. **89**, 093120-1-3 (2006).
18. T. Matsumoto, Y. Anzai, T. Shintani, K. Nakamura, and T. Nishida, "Writing 40 nm marks by using a beaked metallic plate near-field optical probe," Opt. Lett. **31**, 259-261 (2006).

#89303 - $15.00 USD Received 1 Nov 2007; revised 6 Dec 2007; accepted 6 Dec 2007; published 11 Dec 2007

19. K. Kneipp, H. Kneipp, I. Itzkan, R. R. Dasari, and M. S. Feld, "Surface-enhanced Raman scattering and biophysics," J. Phys.: Condens. Matter **14**, R597-624 (2002).
20. C. Sonnichsen, B. M. Reinhard, J. Liphard and A. P. Alivisatos, "A molecular ruler based on plasmon coupling of single gold and silver nanoparticles," Nat. Biotechnol. **23**, 741-745 (2005).
21. S. Y. Park and D. Stroud, "Surface-plasmon dispersion relations in chains of metallic nanoparticles: an exact quasistatic calculation," Phys. Rev. B **69**, pp. 125418-1-7 (2004).
22. W. H Weber and G. W. Ford, "Propagation of optical excitations by dipolar interactions in metal nanoparticle chains," Phys. Rev. B **70**, 125429 (2004).
23. S. A. Maier, M. L. Brongersma, P. G. Kik, and H. A. Atwater, "Observation of near-field coupling in metal nanoparticle chains using far-field polarization spectroscopy," Phys. Rev. B **65**, 193408 (2002).
24. Q. H. Wei, K. H. Su, S. Durant, and X. Zhang, "Plasmon Resonance of Finite One-Dimensional Au Nanoparticle Chains," Nano Lett. **4**, 1067-1071 (2004).
25. K. B. Crozier and E. Togan, "Experimental measurement of the dispersion relations of metal nanoparticle chains," in *Conference on Lasers and Electro-Optics/Quantum Electronics and Laser Science and Photonic Applications Systems Technologies*, Technical Digest (CD) (Optical Society of America 2007) paper QThB4.
http://www.opticsinfobase.org/abstract.cfm?URI=QELS-2007-QThB4
26. K. L. Kelly, E. Coronado, L. L. Zhao, and G. C Schatz, "The optical properties of metal nanoparticles: the influence of the size, shape and dielectric environment," J. Phys. Chem. B. **107**, 668-677 (2003).
27. C. F. Bohren and D. R. Huffman, *Absorption and Scattering of Light by Small Particles* (Wiley, New York, 1983).
28. FDTD software is FullWave from RSoft Design Group, Ossining, New York.
29. A. D. Rakic, A. B. Djurisic, J. M. Elazar and M. L. Majewski, "Optical properties of metallic films for vertical-cavity optoelectronic devices," Appl. Opt. **37**, 5271-5283 (1998).
30. A. Ishimaru, *Electromagnetic Wave Propagation, Radiation, and Scattering* (Prentice Hall, 1991).
31. A. Stratton, *Electromagnetic Theory*, (McGraw Hill, 1941).

1. Introduction

The realization of waveguides with sub-wavelength lateral mode confinement would present a means to miniaturize optoelectronic circuits to nanoscale dimensions. Conventional dielectric waveguides [1] do not offer this possibility, since the minimum beam diameter is determined by the effective wavelength in the core material [2]. This motivated the proposal of an alternative approach, based on chains of closely-spaced metal nanoparticles [3]. Electrodynamic coupling between surface plasmons excited on neighboring nanoparticles enables electromagnetic energy to be transmitted along such structures. This presents an opportunity for shrinking waveguides to sub-wavelength lateral dimensions, since the constituent nanoparticles are only tens of nanometers wide. Nanoparticle chains should allow the propagation of electromagnetic energy around sharp corners with bending radii much smaller than the free space wavelength [4]. Early work on metal nanoparticle chain waveguides predicted significant propagation losses, e.g. 3 dB per 15 nm [5]. However, these estimates have been significantly revised in light of recent theoretical models [6], [7] that predict that longer propagation lengths (amplitude *1/e* decay lengths) are achievable, for example above 5 μm [7]. Metal nanoparticle chains were studied theoretically by Markel in 1993 using the coupled-dipole approach [8]. Since then, in addition to waveguides, a number of applications have been proposed. The surface plasmon modes of nanoparticle arrays were proposed for use in random lasers [9]. Optically-trapped nanoparticle chains were studied by Guillon [10]. The use of nanoparticle chains for sensing [11], sub-wavelength imaging [12], and integrated optics [13] has also been proposed. Li *et al* suggested that a chain of metal nanospheres with different sizes could be used to generate intense local electric fields [14]. Coupling between pairs of nanoparticles also plays a central role in optical antennas [15-18], surface enhanced Raman scattering [19] and molecular rulers [20].

Of critical importance for waveguide applications of metal nanoparticle chains is the dispersion relation $\omega(k)$. The dispersion relation specifies the dependence of the frequency ω on the wavenumber k, and therefore determines the range of frequencies that can propagate in a waveguide. It also determines the group velocities, and attenuation coefficients. Theoretical models of the dispersion relations have been proposed [4, 7, 21, 22].

#89303 - $15.00 USD Received 1 Nov 2007; revised 6 Dec 2007; accepted 6 Dec 2007; published 11 Dec 2007

Experimental observations have been made of the plasmon resonances of nanoparticle chains illuminated at normal [23] and 45˚ [24] incidence. Here, we measure plasmon resonance frequencies using transmission spectroscopy, with the angle of incidence varied from 0 to 75 degrees. This allows the dispersion relation to be mapped over a wide range of *k* values. Surprisingly, our results reveal the presence of a third plasmon mode that was not reported in previous experiments [23,24]. Those experiments reported the existence of one longitudinal and one transverse mode. We recently presented our experimental results at the Conference on Lasers and Electro-Optics [25]. The results represent, to the best of our knowledge, the first experimental measurements of the dispersion relations of chains of closely-spaced metal nanoparticles. In that investigation [25], we compared our results to a basic quasi-static theory. In this paper, we compare the experimental results to a theoretical model that is fully-retarded and includes the effects of radiation damping. The finite size of the nanoparticles is modeled using the Modified Long Wavelength Approximation (MLWA) [26]. In addition, we present a numerical study of the local fields that are created by different plasmon modes.

2. Fabrication of Gold nanoparticle chains

Gold nanoparticle chains are fabricated on glass slides by electron beam lithography, metal evaporation and lift-off. The starting substrate is a glass slide coated with indium tin oxide (ITO) to minimize charging during fabrication. Poly-methyl-methacrylate (PMMA) is spun on and baked. The nanoparticle chain pattern is exposed by electron beam lithography, and the sample is developed. Gold is evaporated to a thickness of 55 nm, with chrome (5 nm) used for adhesion. The PMMA is dissolved in acetone, followed by methanol and then isopropanol. The scanning electron micrographs of Figs. 1(a) and 1(b) illustrate the final result. The total extent of the array of gold nanoparticle chains is 100 μm × 100 μm. The constituent nanoparticles have diameters of ~92 nm, and center-to-center distances of 140 nm along the length of the chain. The spacing between adjacent chains is 300 nm. While coupling between adjacent chains will influence the dispersion relation, we expect that the effect will be small compared to interactions between neighboring nanoparticles (140 nm) in each chain. We expect that the results of our study will be highly representative of the results that would be obtained for isolated chains. This is discussed later in greater detail.

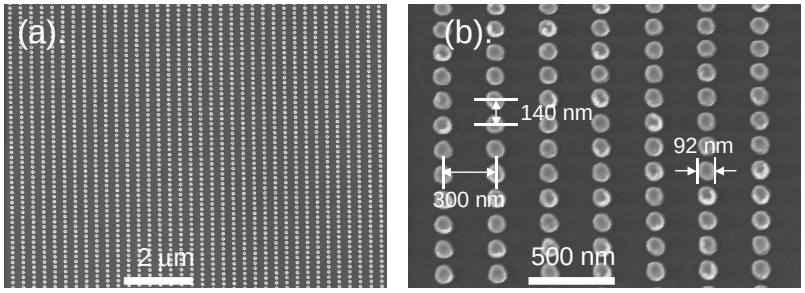

Fig. 1. (a). and (b). Scanning electron micrographs (SEMs) of gold nanoparticle chains. Nanoparticle spacing along chain is 140 nm. Adjacent chains are spaced by 300 nm. Nanoparticle diameter is 92 nm. Gold thickness is 55 nm.

3. Measurement of dispersion relations of Gold nanoparticle chains

To determine the dispersion relations, transmission spectroscopy of fabricated devices is performed with the set-up shown as Fig. 2. The light source is a Xenon lamp, which is focused into an optical fiber. A microscope objective is used to collect light from the optical fiber, which then passes through a polarizer and illuminates the sample. The sample is mounted on a rotation stage. Rotating the sample allows the wavenumber *k* along the nanoparticle chain to be varied, and the resulting wavelength of the plasmon resonance to be measured. The light transmitted through the sample is collected by a microscope objective. An adjustable iris is used at the image plane to collect only the light transmitted through the

#89303 - $15.00 USD Received 1 Nov 2007; revised 6 Dec 2007; accepted 6 Dec 2007; published 11 Dec 2007

nanoparticle chain array. The light passing through the iris is focused into an optical fiber by a microscope objective, and input to an optical spectrum analyzer. The transmission spectra presented here are found by normalizing spectra measured through the nanoparticle chain array by spectra measured through an unpatterned region of the glass slide.

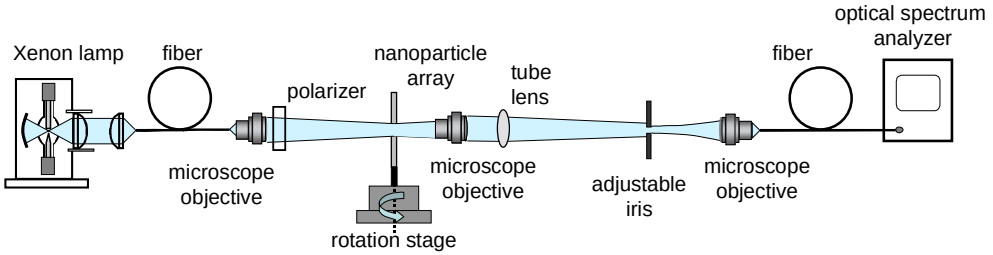

Fig. 2. (color online) Experimental set-up used for transmission spectroscopy of metal nanoparticle chains with the angle of incidence varied.

Adjustment of the polarizer allows transmission spectra to be measured with s-polarized (Fig. 3(a)) and p-polarized (Fig. 3(b)) illumination. The sample is oriented such that the axis of the nanoparticle chain, along which the nanoparticles are spaced by 140 nm, is in the plane of incidence. This is shown in the insets of Figs 3(a) and 3(b). The angle of incidence θ is varied from 0 to 75˚, in steps of 5˚. The spectra are vertically offset for clarity, by 0.05 per spectrum, starting with zero offset for normal (0˚) incidence. The dips in the spectra correspond to the plasmon resonance wavelengths of the nanoparticle chains. At these wavelengths, plasmon oscillations in the nanoparticle chains reach their maximum amplitudes. The increased scattering and absorption that result lead to transmission minima. It can be seen from Fig. 3(a) that s-polarized illumination couples to a single mode (transverse, denoted "T1"). Increasing the angle of incidence results in the transmission spectra probing portions of the dispersion relation with longer wavevectors (k). For the transverse mode T1, the plasmon wavelength red-shifts as the wavevector (k) is increased, as discussed later in greater detail. P-polarized illumination couples to a single mode (longitudinal, denoted "L") at normal incidence, with an additional mode (transverse, denoted "T2") coupled to at large angles of incidence. The plasmon wavelength of the longitudinal mode L blue-shifts as the wavevector (k) is increased. This is discussed later in detail. To the best of our knowledge, mode T2 has not been previously observed. Previous experimental observations of the plasmon resonances of metal nanoparticles chains were made either at normal [23] or 45˚ [24] incidence, and therefore did not excite this mode appreciably.

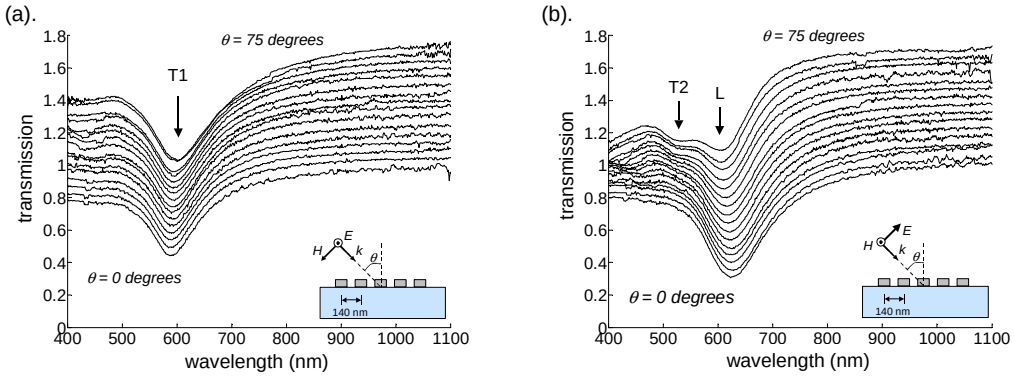

Fig. 3. (color online) Transmission vs wavelength of gold nanoparticle chain arrays. The angle of incidence is varied from 0° to 75°, in steps of 5°. The spectra are vertically offset for clarity. a). S-polarization, exciting transverse mode T1. b). P-polarization, exciting longitudinal mode L and transverse mode T2.

#89303 - $15.00 USD Received 1 Nov 2007; revised 6 Dec 2007; accepted 6 Dec 2007; published 11 Dec 2007

4. Physical interpretation of plasmon modes

The dispersion and coupling behavior of the modes of metal nanoparticle chains exhibited in Fig. 3 can be understood by modeling the chains as systems of coupled electric dipoles [4]. For noble metal nanoparticles with diameters much smaller than the illumination wavelength, the excitation of surface plasmons produces oscillating dipole fields [27]. We begin by considering the modes of metal nanoparticle chains and their coupling behavior. Modes of metal nanoparticles chain fall into two categories, depending on the orientation of the dipole moments of the constituent nanoparticles. In the longitudinal mode, illustrated schematically in Fig. 4, the dipole moments are oriented along the direction of the chain. The transverse modes have their dipole moments oriented perpendicular to the chain. Previous theoretical models [3,4,7,21,22] of nanoparticle chains consider them to consist of spheres embedded in a homogeneous medium. In those models, therefore, the nanoparticles chains have one longitudinal and two, degenerate, transverse modes. However, in the experimental realization presented in this Letter, as well as previous reports [23, 24], metal nanoparticle chains are fabricated on glass substrates by electron beam lithography. We therefore expect that these nanoparticle chains will exhibit one longitudinal mode and two distinct transverse modes. In transverse mode T1, the dipole moments are oriented in the plane of the substrate. In addition to T1, we expect a second transverse mode T2, in which the dipole moments are oriented normal to the substrate. Due to the non-spherical nature of the nanoparticles, and the fact that the local field distribution of the two modes will be different since the nanoparticles are situated at the interface between materials with different dielectric constants, we expect that modes T1 and T2 will be non-degenerate. Mode T2 is discussed in greater detail below with the aid of numerical simulations. In order for a mode to be coupled to, the electric field of the illumination must have a component oriented along the direction of the dipole moments of the metal nanoparticles. As illustrated in Fig. 3(a), we expect that transverse mode T1 will be therefore coupled to with s-polarized illumination. Similarly, we expect that p-polarized illumination (Fig. 3(b)) will couple to both longitudinal L and transverse T2 modes. However, for appreciable coupling to mode T2, a large angle of incidence should be necessary. Mode T2 should not be coupled to at normal incidence. Similarly, coupling to mode L and, correspondingly, the amplitude of the dip in the transmission should steadily decrease as the angle of incidence is increased. These predictions are consistent with the experimental results of Fig. 3.

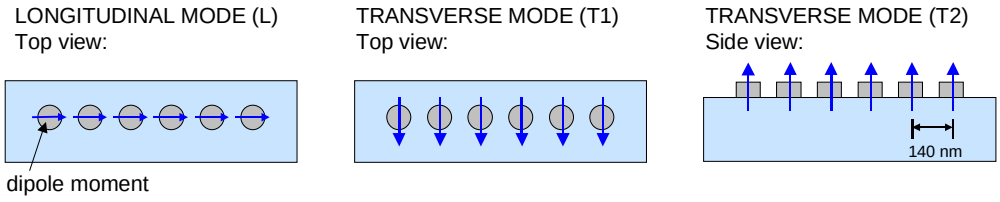

Fig. 4. (color online) Orientation of dipole moments of metal nanoparticles in longitudinal and transverse modes

In order to understand the nature of mode T2, we perform finite difference time domain (FDTD) calculations of the internal field distributions of the gold nanoparticles [28]. As shown in Fig. 5, the metal nanoparticles are modeled as gold cylinders with diameters of 90 nm and heights of 55 nm. A unit cell, consisting of a single gold nanoparticle, is modeled, and periodic boundary conditions are used to account for the periodic nature of the nanoparticle array. The spacing between nanoparticles along the chain is 140 nm, and the spacing between adjacent chains in 300 nm, matching the parameters of fabricated structures. A grid spacing of 5 nm at and near the particles is employed. The complex refractive index of the gold is taken from Reference [29]. The incident illumination is a p-polarized plane wave

#89303 - $15.00 USD Received 1 Nov 2007; revised 6 Dec 2007; accepted 6 Dec 2007; published 11 Dec 2007

introduced from the glass side. Periodic boundary conditions are applied at the ±*x* and ±*y* boundaries. Perfectly matched layers are applied at the ±z boundaries.

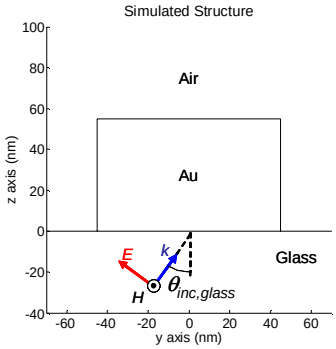

Fig. 5. (color online) Cross sectional view of FDTD simulation domain, consisting of unit cell that encloses a single gold nanoparticle on a glass substrate. P-polarized plane wave illumination is employed.

To check the accuracy of our technique, we calculate the far-field transmission spectrum, allowing comparison with experiment. To do this, we carry out a number of FDTD simulations. In each simulation, a pulse covering the spectral region of interest is launched at a single k_y value, with k_x fixed at zero. By interpolating the simulation results, we obtain the far-field transmission spectrum for p-polarized illumination at an incident angle $\theta_{inc,\,glass}$ of 35° from the normal to the glass-air interface. This corresponds to a transmitted angle of 60°. The results are shown as Fig. 6, together with transmission measured on the fabricated nanoparticle array. It should be noted that no fitting parameters are used in the comparison between simulation and experiment. From Fig. 6, it can be seen that the FDTD simulations are in very good agreement with the experimental results. The dips in the transmission, as well as the overall shape, of the FDTD-calculated spectrum are in good agreement with experiments. This confirms the accuracy of our FDTD modeling method.

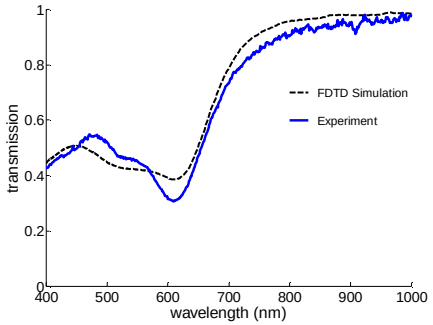

Fig. 6. (color online) Transmission spectra of gold nanoparticle array: FDTD simulation and experiment. P-polarized illumination is used, from the glass side at $\theta_{inc,\,glass}$ = 35° from the normal to the glass-air interface.

We now employ FDTD simulations to understand the nature of modes L and T2, which manifest themselves as dips in the transmission spectra of Fig. 6. In the numerical simulations, these modes occur at free space wavelengths of 613.5 nm and 512.8 nm, respectively, as found from the peaks of the FDTD-calculated absorption spectra (data not shown). We begin by considering the L mode. We calculate the internal electric field distribution of the nanoparticle when it is excited with continuous wave (CW) illumination at λ_0 = 613.5 nm. The p-polarized plane wave is incident from the glass at $\theta_{inc,glass}$ = 35°. In Fig. 7, the instantaneous internal electric fields are plotted for a cross section through the

#89303 - $15.00 USD Received 1 Nov 2007; revised 6 Dec 2007; accepted 6 Dec 2007; published 11 Dec 2007

nanoparticle in the *yz* plane with $x = 0$. The fields are plotted at five instants over half an optical cycle, namely at $t = \{0, T/8, T/4, 3T/8, T/2\}$, where T is the period. From Fig. 7, it can be seen that the fields are predominantly oriented along the *y* axis. The fields oscillate from being oriented in the $+y$ direction at $t=0$, to the $-y$ direction at $t=T/2$, and so forth. At $t=T/4$, the field amplitudes are smaller, and are mainly oriented along the *z* axis. The calculated field distributions indicate that oscillating charges accumulate at the edges and corners of the nanoparticle, as evidenced by the large divergence of the electric field at those locations. The calculated field distributions are in agreement with our interpretation (Fig. 4) of this being a longitudinal mode, in which the dipole moments of the nanoparticles are oriented along the direction of the chain.

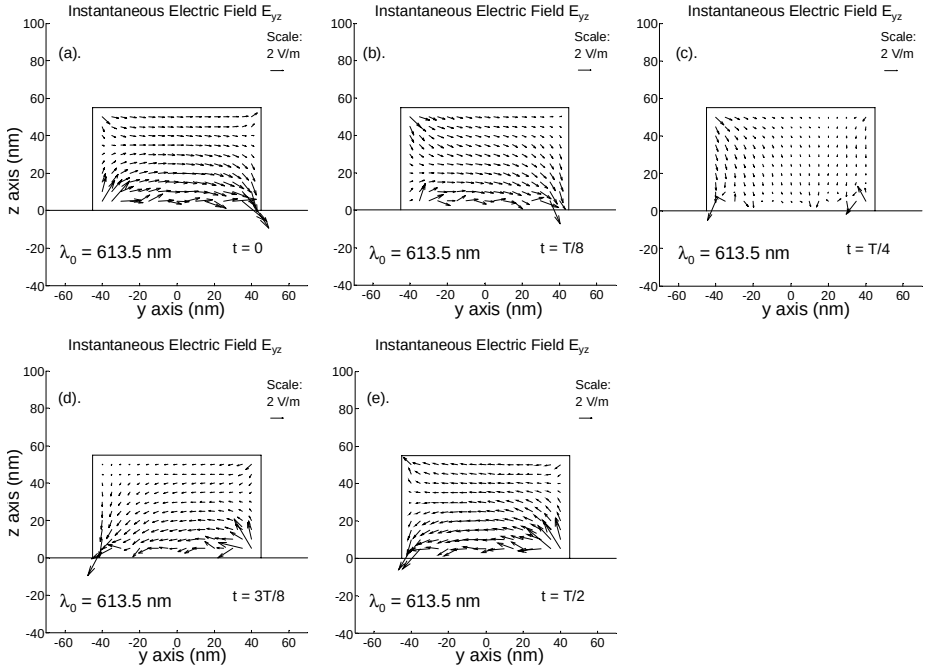

Fig. 7. Internal instantaneous electric field on cross section through gold nanoparticle (*yz* plane, $x = 0$) illuminated at $\lambda_0 = 613.5$ nm. Illumination is p-polarized plane wave (amplitude 1 V/m), incident from the glass side at $\theta_{inc,\,glass} = 35°$ from the normal to the glass-air interface. Instantaneous electric field at time a). $t=0$, b). $t=T/8$, c). $t=T/4$, d). $t=3T/8$ and e). $t=T/2$, where T = period.

We now consider the T2 mode. As before, a p-polarized plane wave is incident from the glass at $\theta_{inc,glass} = 35°$, however in this case $\lambda_0 = 512.8$ nm. In Fig. 8, the instantaneous internal electric field distributions are plotted on a cross section through the *yz* plane at $x = 0$.. It can be seen that the fields exhibit a strong component of polarization in the *z* direction, especially at $t = 0, T/2$, and so forth. There is also an appreciable component of the field in the y-direction, especially at $t = T/8, 5T/8$, and so forth. This is most likely due to the excitation of both the L and T2 modes, with a phase difference between them of $\sim\pi/2$. While the L mode is centered at $\lambda_0 = 613.5$ nm, the wide bandwidth of the plasmon resonance leads to appreciable excitation even at $\lambda_0 = 512.8$ nm. From the calculated field distributions, we interpret T2 as a mode in which the dipole moments of the constituent nanoparticles are oriented perpendicular to the direction of the chain, and normal to the substrate. This is consistent with model proposed in Fig. 4.

#89303 - $15.00 USD Received 1 Nov 2007; revised 6 Dec 2007; accepted 6 Dec 2007; published 11 Dec 2007

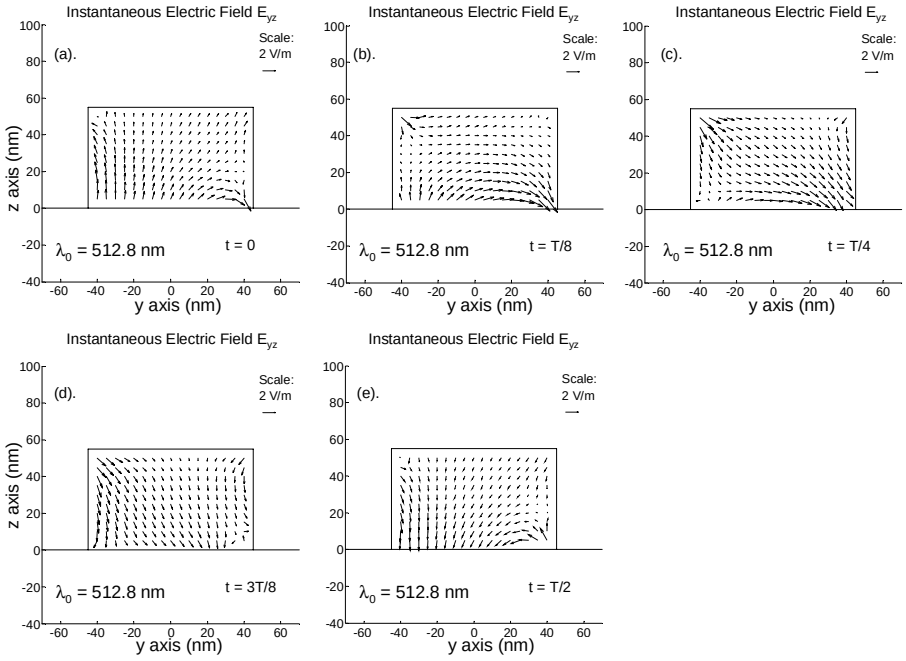

Fig. 8. Internal instantaneous electric field on cross section through gold nanoparticle (*yz* plane, $x = 0$) illuminated at $\lambda_0 = 512.8$ nm. Illumination is p-polarized plane wave (amplitude 1 V/m), incident from the glass side at $\theta_{inc,\,glass} = 35°$ from the normal to the glass-air interface. Instantaneous electric field at time a). $t=0$, b). $t=T/8$, c). $t=T/4$, d). $t=3T/8$ and e). $t=T/2$, where T = period.

5. Dispersion relations

From the transmission spectra of Fig. 3, the dispersion relations of the plasmon modes can be determined. The plasmon frequencies (ω) are found from the positions of the transmission minima (dips) in the measured spectra. The in-plane k vectors are then found from:

$$k_{in-plane} = \frac{\omega}{c}\sin\theta \qquad (1)$$

where θ is the angle of incidence, as shown in Fig. 3. The dispersion relations of the *L* and *T1* modes found in this way are plotted as Fig. 9. Each symbol represents a data point found from the position of a transmission minimum (dip) in the spectra of Fig. 3. We fit each spectrum with a fifth order polynomial, in a 100nm bandwidth about the dip position, and find the minimum of the fitted curve. In earlier work [25], we found the plasmon resonance frequencies from the minima of the experimental transmission spectra. However, we find that fitting each spectrum with a polynomial is effective at mitigating against the effects of experimental noise. Dispersion relations, calculated using the fully-retarded model of Weber and Ford [22], are also shown. In this fully-retarded model, the full time-dependent fields of an oscillating dipole are used. Interactions between dipoles contain terms varying as $1/r$, $1/r^2$ and $1/r^3$. We make some modifications to the model of Weber and Ford [22]. We account for the non-spherical nature of the nanoparticles by modeling them as ellipsoids rather than spheres. We use the experimental values for the optical constants of gold [29], rather than the Drude model. Lastly, we employ the Modified Long Wavelength Approximation (MLWA) [26] to account for the shift in plasmon frequency and polarizability due to the finite size of nanoparticles.

#89303 - $15.00 USD Received 1 Nov 2007; revised 6 Dec 2007; accepted 6 Dec 2007; published 11 Dec 2007

In calculating the dispersion relations, we assume that the axis of the nanoparticle chain is along the *y* direction, with the spacing between nanoparticles being d_y. The semi-axes of the ellipsoids along the *(x,y,z)* axes are *(a,b,c)*. From Fig. 1(b), it can be seen that the nanoparticles have diameters of ~92 nm. The gold thickness is 55 nm. Therefore, we choose $a=b=$ 46 nm, and c=27.5 nm in our model. Taking the x-axis as an example, the nanoparticle polarizability is given by:

$$\alpha_{0,x} = \frac{\varepsilon_r - \varepsilon_b}{\varepsilon_b + L_x(\varepsilon_r - \varepsilon_b)} \frac{abc}{3} \tag{2}$$

where ε_r and ε_b are the permittivities of the nanoparticle and background, respectively. Similar expressions exist for the nanoparticle polarizability along the *y* and *z* axes. The geometrical factor L_x is given by [30]

$$L_x = \frac{abc}{2} \int_{s=0}^{\infty} \frac{1}{s+a^2} \left((s+a^2)(s+b^2)(s+c^2) \right)^{-1/2} ds \tag{3}$$

In our case $a = b$, so we also have $L_x = L_y$.

To account for the effects of retardation, it is necessary to include the effect of radiative damping in the polarizability. In addition, the finite size of the nanoparticles means that there will be a depolarization of the radiation across the particle surface. This phenomenon is known as dynamic depolarization and causes red-shifting of the plasmon resonance with increasing particle size. The theory that describes these effects is sometimes known as the MLWA [26]. The polarizability is modified to be:

$$\alpha = \left(\frac{1}{\alpha_0} - i\frac{2}{3}k^3 - \frac{k^2}{a} \right)^{-1} \tag{4}$$

The second term in the brackets of Eq. (4) describes radiative damping, and the third term describes dynamic depolarization.

The model employed here, as well as other models that have been reported [4, 7, 21, 22], assumes that the nanoparticles are situated in a homogeneous medium. However, in the experiments we report here, as well as those of Refs. [23, 24], the nanoparticles are situated at the interface between two media with different dielectric constants, namely glass and air. The development of a theoretical fully-retarded model for surface plasmons on metal nanoparticle chains at the interface between two media would be of great value. In the current absence of such a model, we calculate the two sets of dispersion relations. In the first set, the nanoparticles are assumed to be in air. In the second set, the nanoparticles are assumed to be in a homogeneous glass medium, with a refractive index of 1.51. The calculated dispersion relations are shown as Fig. 9. In Fig. 9(a), the experimental results for the T1 and L modes are plotted along with the calculated dispersion curves. In Fig. 9(b), the calculated dispersion curves for the T2 modes are plotted. It should be noted that no fitting parameters are used in the theoretical model. The model employed [22] solves for the discrete normal modes of a set of *N* nanoparticles. In the limit of *N* being large, the normal mode frequencies form a continuous distribution, corresponding to the dispersion relation. This approach is analogous to solving for a chain of coupled oscillators, where each oscillator is coupled to all others. In Fig. 9, we employ a chain of 60 nanoparticles and solve for the plasmon frequencies.

#89303 - $15.00 USD Received 1 Nov 2007; revised 6 Dec 2007; accepted 6 Dec 2007; published 11 Dec 2007

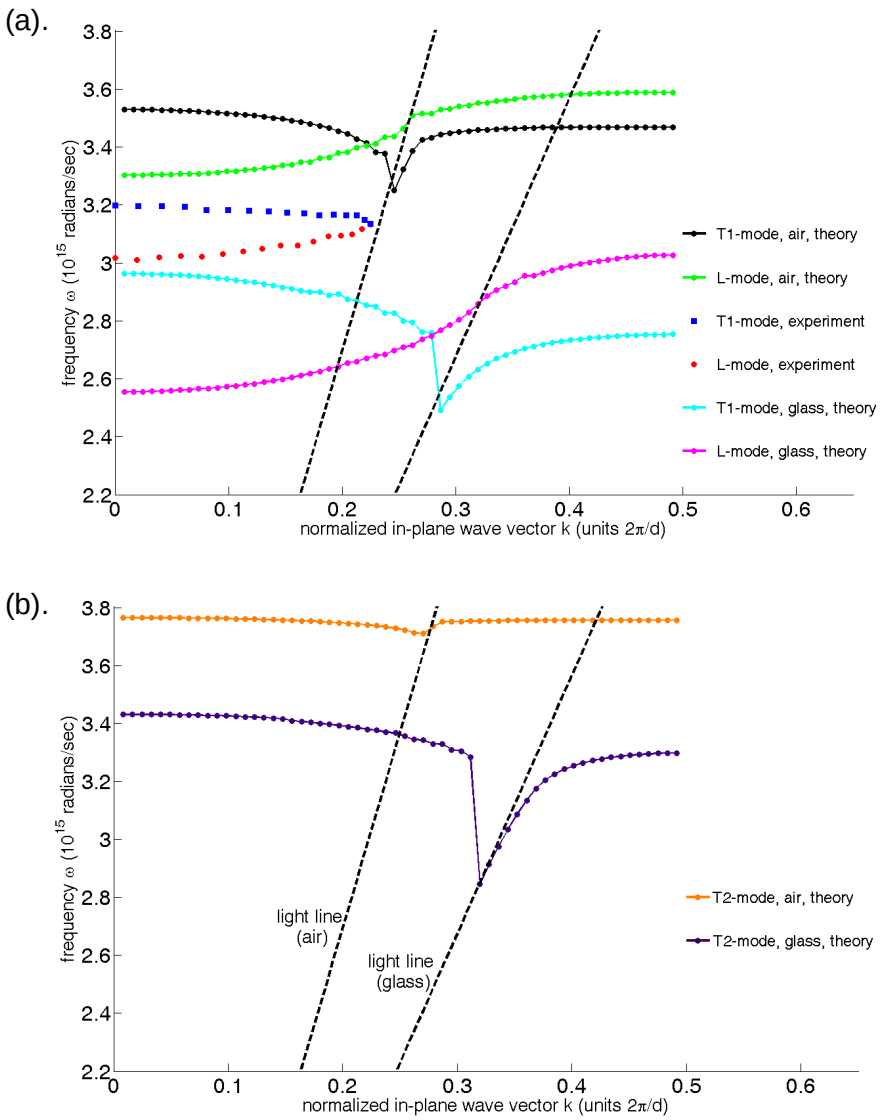

Fig. 9. (color online) Surface plasmon dispersion relationship of metal nanoparticle chains. Theoretical curves are based on a fully-retarded model for the cases of nanoparticles in air, and nanoparticles in a homogeneous glass medium. a). Longitudinal (L) and first transverse (T1) modes: theory and experiment. b). Second transverse mode (T2): theory

From Fig. 9(a), it can be seen that the experimental results for the T1 and L modes occur in a frequency range that is in between the theoretical dispersion relations for nanoparticles in air and in glass. From Fig. 3(b), it can be seen that the transmission dips associated with the T2 mode are not as deep as those of the T1 or L modes. Apart from the transmission spectrum obtained for the largest angle of incidence (75°), the spectral features associated with the T2 mode do not exhibit local minima. Therefore, unlike the T1 and L modes, for the T2 mode we do not extract the resonance frequencies from the experimental data for the purpose of comparison to theory. Instead, as shown in Fig. 10, we re-plot the transmission spectra of Fig. 3(b) for the largest angles of incidence, indicating the theoretical predictions for the positions of the T2 modes for the cases of nanoparticles in air, and nanoparticles in glass. The theoretical predictions are extracted from the data plotted as Fig. 9(b). From Fig.

#89303 - $15.00 USD Received 1 Nov 2007; revised 6 Dec 2007; accepted 6 Dec 2007; published 11 Dec 2007

10, it can be seen that the T2 mode experimental results occur in a frequency range the lies between the two theoretical dispersion calculations.

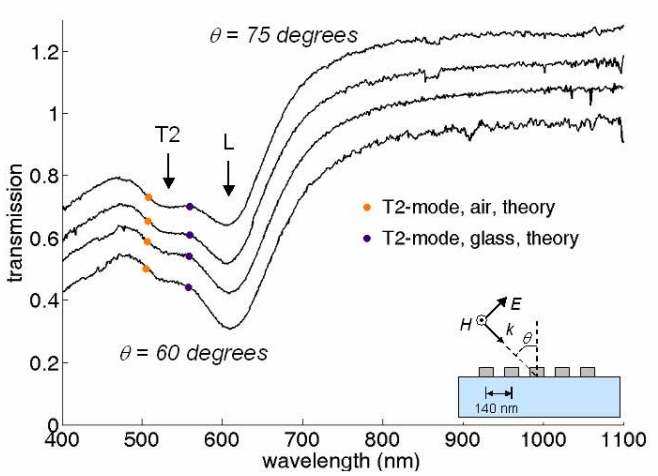

Fig. 10. (color online) P-polarized transmission spectra, with angle of incidence ranging from 60° to 75°, in steps of 5°. Spectra are vertically offset for clarify. Orange symbols: theoretical positions of T2 mode for nanoparticles in air. Purple symbols: theoretical positions of T2 mode for nanoparticles in glass.

Our theoretical calculations predict that nanoparticles in a glass medium are considerably red-shifted, compared to nanoparticles in air. It is therefore consistent that the experimental results, in which the nanoparticles are situated at the interface between an air/glass medium, occur in a frequency range between the theoretical dispersion relations for nanoparticles in air and glass. We can conclude from Figs. 9 and 10 that the fully retarded dispersion model for nanoparticles in a homogeneous medium predicts dispersion relations that are qualitatively correct, as evidenced by their consistency with the experimental results. However, the results suggest that quantitative modeling will only be possible with a theory that accounts for the fact that the dipoles are at an interface between air and glass.

An interesting question is the influence of adjacent nanoparticle chains upon the measured dispersion relations. The induced dipole moment of a nanoparticle is equal to its polarizability $\alpha(\omega)$ multiplied by the local electric field, which is due to the fields from the other nanoparticles. The effects of coupling between adjacent chains can therefore be quantified by comparing the contribution to the electric field at a nanoparticle from a nearest neighbor within the chain to the contribution from a nearest neighbor of an adjacent chain. The electric field generated by a single dipole $\boldsymbol{p}\ exp(-i\omega t)$, oscillating with frequency ω is given by [31]:

$$E(p,r,\omega)=\frac{1}{4\pi\varepsilon}\left[\left(1-\frac{i\omega r}{v}\right)\frac{3(\hat{r}\cdot\vec{p})\hat{r}-\vec{p}}{r^3}+\frac{\omega^2}{v^2}\frac{\vec{p}-(\hat{r}\cdot\vec{p})\hat{r}}{r}\right]\times e^{i\omega r/v-i\omega t} \qquad (5)$$

where $\hat{r}$ is the unit vector pointing from the dipole to the field point at distance r, n is the refractive index of the medium, $\varepsilon=n^2\varepsilon_0$ is the permittivity of the medium surrounding the dipole, and $v=c/n$ is the speed of light in the medium. For the purposes of calculation, we assume that the wavelength is λ_0 = 600 nm, and that the medium is free space. The spacing between nanoparticles in a chain is taken as 140 nm and the spacing between adjacent chains is 300 nm, matching the parameters of fabricated devices. Let us first consider the longitudinal mode. From Eq. (5), we find that the magnitude of the electric field at a nanoparticle from a nearest neighbor dipole in the chain is ~3.7 times that of the field from the nearest neighbor dipole in an adjacent chain. For the transverse mode, we find that the

#89303 - $15.00 USD Received 1 Nov 2007; revised 6 Dec 2007; accepted 6 Dec 2007; published 11 Dec 2007

magnitude of the electric field at a nanoparticle from a nearest neighbor dipole in the chain is ~2.8 times that of the field from the nearest neighbor dipole in an adjacent chain. Also, it should be noted that the wavevector *k* under consideration is that along the chain, giving the phases of the dipole moments of the nanoparticles in each chain. The wavevector *k* between adjacent chains is not varied, meaning that the phase of the dipole moment of each nanoparticle is the same as that of its nearest neighbors in adjacent chains. We conclude that while coupling between adjacent chains influences the dispersion relations, we expect them to be dominated by interactions between neighboring nanoparticles in each chain. This confirms that our experimental results are highly representative of the dispersion relations of isolated chains.

The experimental results presented here are obtained using transmission measurements, and therefore probe the portion of the dispersion relation above the light line of air. While experimental and theoretical results are in qualitative agreement in this region, we expect that this will not be the case below the light line. We expect that the transition from transmission to total internal reflection will be accompanied by major changes in the coupling between nanoparticles. We intend to carry out further experiments and modeling in this portion of the dispersion relation. Our results motivate the development of a theoretical model that accounts for the fact that the nanoparticles are situated at the interface between two dielectric media.

6. Conclusions

We have measured the dispersion relations of the surface plasmon modes of metal nanoparticle chains. In addition to one longitudinal and one transverse mode, the experimental spectra reveal the existence of a third mode, which had not been previously reported. FDTD simulations revealed that this mode is transverse in nature, with the dipole moments of constituent nanoparticles oriented normal to the substrate. The experimental dispersion relations were found to be in reasonable qualitative agreement with the results of the fully-retarded point dipole model. The results demonstrate the dispersive nature of metal nanoparticle chains, which will be important in future waveguide applications.

Acknowledgments

This work was supported by the Defense Advanced Research Projects Agency (DARPA), Draper Laboratory, and the Nanoscale Science and Engineering Center (NSEC) at Harvard, which is funded by the National Science Foundation (NSF). Fabrication work was carried out in the Center for Nanoscale Systems (CNS) at Harvard, which is also funded by the NSF. The authors acknowledge technical support from RSoft Design Group. The authors thank two anonymous reviewers, whose criticisms of an earlier version on this manuscript are greatly appreciated.

#89303 - $15.00 USD Received 1 Nov 2007; revised 6 Dec 2007; accepted 6 Dec 2007; published 11 Dec 2007